Birds of a Feather?

Glenn M. Thurman

Cuyamaca College, El Cajon, California

Abstract:

A wide double, selected for components of similar parallax, radial velocity, proper motion and spectral-luminosity class, was observed and measures of separation and position angle are reported and compared with historical data. The question of boundedness is investigated by comparing the gravitational potential energy of the system with the relative kinetic energy of the components. The possibility that the components are co-chemical/common-origin is examined by comparing instrumental Stromgren m_1 indices of the components, measured here.

1. Introduction

In this paper I examine a pair of stellar birds that are apparently flocking together, judging from Gaia data, and may even be bound, but are they of a feather? The pair in question: 16265-0042BVD 118.

Measures of position angle and separation are presented and compared with historical data.
Also presented are data from Harshaw's (2018) table, which shows this pair are exactly the same distance from the Sun, to within measurement error, and have nearly the same proper motion and radial velocity – suggestive of a bound system.

We will see from a comparison of the kinetic energy of the primary (with respect to the secondary) and the gravitational potential energy of the system, that the answer to the question of boundedness is *maybe*.

Stromgren photometry is employed to determine if the system is co-chemical. If so, it is probable that the components are of common origin, formed together, and are a bound system (though common origin alone is not proof of boundedness).

2. Target Selection

The Washington Double Star Catalog (WDS; Mason 2017) and Harshaw's (2018) table were scoured for late-type main sequence pairs of equal, or near equal, spectral type, distance, proper motion and radial velocity. Of those, only one pair was suitably positioned for observing, bright enough for intermediate band Stromgren filters, and of separation great enough for photometry and astrometry. WDS data for the selection is presented in Table 1. Gaia DR3 data for the selection is presented in Table 2. Harshaw's table was used for the search, but GAIA DR3 data in Table 2 were taken directly from the GAIA archive, not Harshaw's table.

Table 1. WDS Data for WDS 16265-0042BVD 118.

Star	Sp./Lum	m_v	PA, θ (deg)	Sep, ρ (arcsecs)	2000 Coordinates
Pri.	K0	10.39			16 26 28.65 -00 42 21.2
Sec.	K2V	10.75	239	21.82	

Table 2. Gaia DR3 data for WDS 16265-0042BVD 118

Star	Para (mas)	Para err (mas)	RV km/s	RV err km/s	PM ra (mas/yr)	PM ra err (mas/yr)	PM dec (mas/yr)	PM dec err (mas/yr)	PM (mas/yr)
Pri.	15.35	0.01980	-32.96	0.5859	-45.19	0.01877	2.640	0.01324	45.27
Sec	15.36	0.02092	-34.40	1.351	-44.12	0.01972	2.178	0.01421	44.17

Calculations in this work use data (i.e., spectral-luminosity class, apparent magnitude, separation angle, parallax, radial velocity, proper motion, and associated errors) from Tables 1 and 2.

3. Observations and Reduction

The observations were made using a Meade LX200 16-inch f/10 reflecting telescope located at Gregory T. Thurman Memorial Observatory, in the foothills of East County San Diego, California, situated at about 2600 feet, under moderately dark skies.

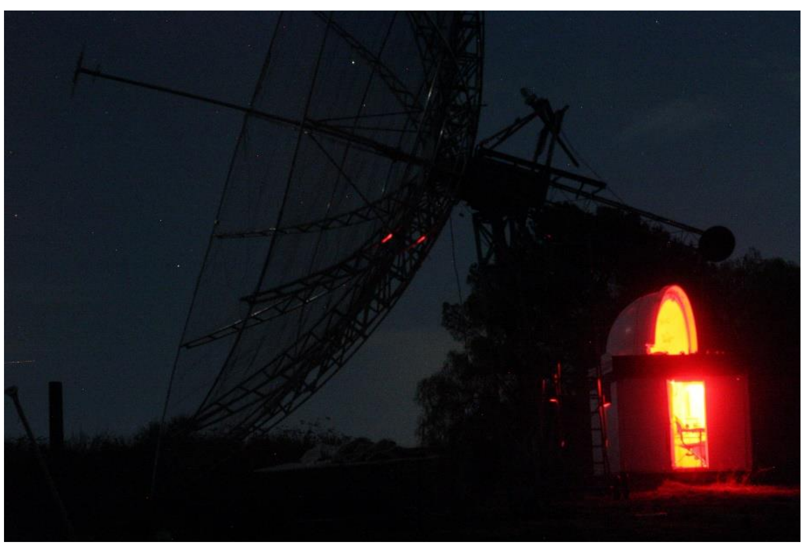

Gregory T. Thurman Memorial Observatory, optical and radio.

The CCD imaging was accomplished using an SBIG STF-8300M monochrome camera, with a KAF-8300 CCD and 1.4-micron square pixels. Images were taken through the vby filters of the Stromgren four-color system. All images were flat-fielded and dark subtracted. The double star astrometry utility of the MPO Canopus software was used for the measures of separation and position angle.

4. Astrometry

Separation, ρ, and position angle, θ, were measured on four Stromgren y-filter-images, using MPO Canopus. The averages of the measures, along with standard errors, were: ρ = 21.81 arcseconds, s.e. = 0.007 arcseconds; θ = 238.85 degrees, s.e. = 0.037 degrees.

Presented in Figures 1 and 2 are Cartesian plots of the motion of the secondary star with respect to the primary, using the combined data, present and historical (WDS). The x and y axis scales are equal for each graph. The "Zoom OUT" graph gives a small-scale view of the data and the location of the primary (represented by a cross). The "Zoom IN" graph gives a large-scale view of the data, with the primary position far off the graph. For each Cartesian plot, the x and y coordinates are given by Equations 1 and 2:

Equation 1. $x = \rho \sin \theta$

Equation 2. $y = \rho \cos \theta$,

where ρ equals the separation in arcseconds, θ equals the position angle in degrees, East is in the positive x direction, and North is in the negative y direction.

No orbital motion is apparent in the figures, only noise. This pair are very far apart.

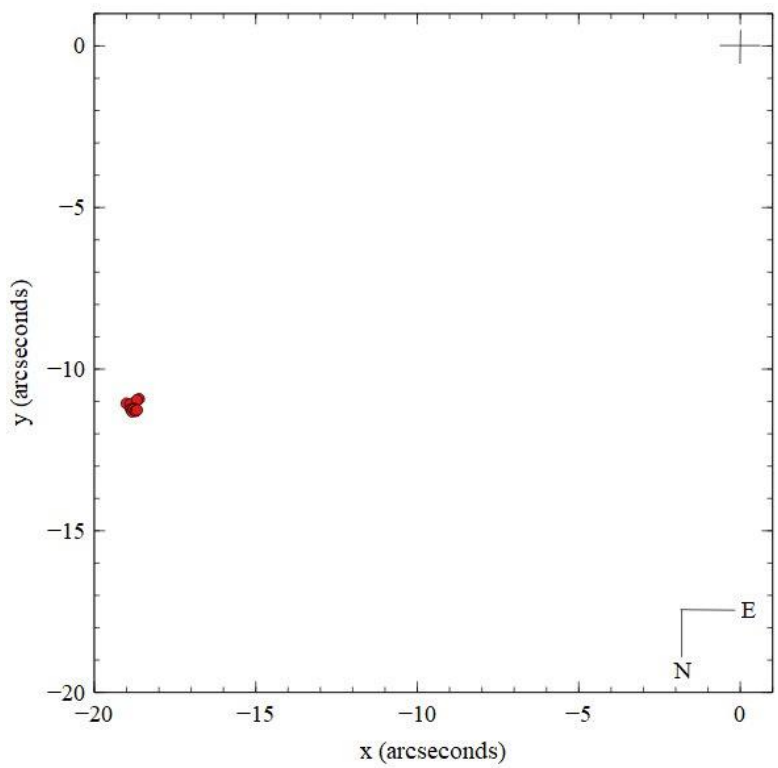

Figure 1. WDS 16265-0042BVD 118 y vs. x ZOOM OUT.

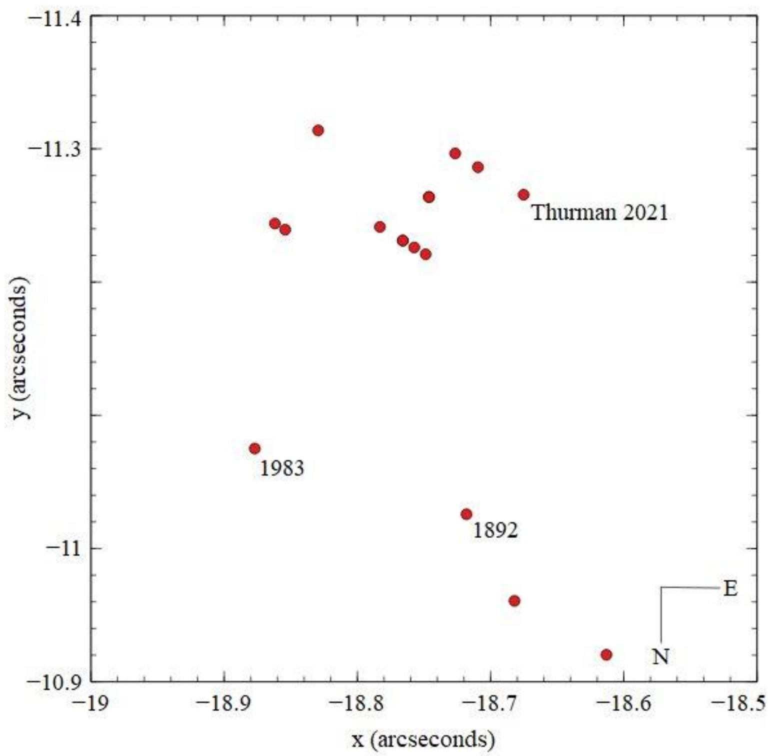

Figure 2. WDS 16265-0042BVD 118 y vs. x ZOOM IN.

5. Dynamics

The distance between the components is given by Equation. 3:

Equation 3 $s = r\rho,$

where s is the distance between the stars, r is the distance of the system from the Sun, and ρ is the angular separation in radians. The formula is accurate for small ρ, such as the typical separation angles in double star work. Taking r = 65.12 parsecs (reciprocal of the Gaia parallax in arcseconds; not milliarcseconds!), ρ = 21.82 arcseconds / (206265 arcseconds per radian), and plugging into Equation 3 yields s = 0.006896 parsecs or 1425 A.U. That's 36 times the Pluto-Sun distance. Given enough time, orbital motion might show itself, if it is a bound system. How much time?

Newton's modification of Kepler's Third Law is given by Equation. 4:

Equation 4 $M_1 + M_2 = a^3 / P^2,$

Where M_1 and M_2 are the masses of star 1 and star 2, in solar masses, respectively, a is the semimajor axis of the system in AU, and P is the period in years. Assuming circular orbits (which is probably wrong, but we know nothing about the orbits and cannot do much else), we can use Equation 4 to get some idea of how large the period might be.

The semimajor axis of a system of two stars in circular orbits about a common center of mass is the sum of the semimajor axes of the two orbits, which is the sum of the radii of circular orbits, which is just the space separation (Calculated above, for the pair under study, using Equation 1: s

= a = 1425 AU.). Next, we need the masses, which we will find using a main sequence, mass-spectral type calibration.

The spectral type of the primary, and spectral-luminosity class of the secondary, as reported in the WDS catalog, are K0 and K2V. The luminosity class of the K0 star is not given. We can use the WDS V (visual) magnitudes and the distances from Gaia parallaxes to find the absolute magnitudes of the pair, which will tell us if the two stars are on the main sequence. If they are indeed both main sequence stars, we can easily look up their masses given their spectral types. The distance modulus is given by:

Equation 5 $$m_v - M_v = 5 \log_{10}(d) - 5,$$

where m_v is the apparent visual magnitude, M_v is the absolute visual magnitude and d is the distance in parsecs.

The distance from Gaia parallax (Table 2) is:

d = 1/[parallax (arcsecs)] = 65.12 parsecs for both primary and secondary,

From Table 1, the visual magnitudes are:

m_v = 10.39 for the K0 primary,

m_v = 10.75 for the K2 secondary.

Plugging the above values of m_v into Equation 5 and solving for M_v yields M_v = 6.32 for the K0 primary and M_v = 6.68 for the K2 secondary. B-V for a K0 star is about 0.82 and for a K2 star is about 0.88. Plotting the absolute magnitudes and B-V color indices on an HR diagram places these two stars firmly on the Main Sequence.

If the WDS spectral types were wrong, or the luminosity class for the K0 star was anything other than V, or the WDS apparent magnitudes were wrong, it is likely the pair would appear anywhere on the HR diagram BUT the main sequence. We therefore adopt the spectral types as correct (Indeed, Sinachopoulos et. al. (1992) write: "…the so often criticized spectral types listed in WDS turned out to be better than often claimed."), the K0 luminosity class as V, and the WDS V (visual) magnitudes as reliable.

Interstellar absorption is not an issue. The rule of thumb is that there are about 2 magnitudes of dimming in the optical band per kiloparsec of distance, due to interstellar absorption. For the distances involved here, the dimming in apparent visual magnitude would therefore be about 0.1 magnitude for each star, which translates to 0.1 magnitude dimming in absolute magnitude for each star. That is not nearly enough to change our conclusions in the previous two paragraphs.

From the main sequence mass-spectral type relation (e.g., Zombeck 1990), the inferred mass of a K0V star is about 0.78 solar masses, and that of a K2V star is about 0.74 solar masses. We now have everything we need to estimate the period.

Plugging these masses into Equation. 2, along with a = 1425 AU (calculated above), and solving for P, yields P = 43631 years. That's a guess based on a circular orbit. It will be a long time before astrometry measures show any evidence of orbital motion, if indeed there is any orbital motion. Nevertheless, the similarities between these two stars in terms of distance, proper motion and radial velocity are reason enough to probe a bit deeper. Energy considerations may light the way.

For the system to be bound,

Equation 6 $$\Delta v_{rel} < \Delta v_{\mathrm{esc}}$$

where Δv_{rel} is the relative velocity between the two components, and Δv_{esc} is the escape relative velocity, that is, the relative velocity above which the components will overcome their mutual gravitational attraction and move to infinite separation.

The relative velocity Δv_{rel} is the magnitude of the vector sum of the relative radial, and relative tangential, velocities, and is given by,

Equation 7 $$\Delta v_{rel} = \sqrt{\Delta v_{rad}^2 + \Delta v_{tan}^2}$$

Where Δv_{rad} is the relative radial velocity between the two components, and Δv_{tan} is the relative tangential velocity between the two components.

The escape relative velocity is given by

Equation 8 $$\Delta v_{\mathrm{esc}} = \sqrt{\frac{2GM_{Tot}}{R}}$$

Where G is the gravitational constant, M_{Tot} is the total mass of the system, and R is the separation between components. Equation 8 is a well-known result (e.g., Rica 2011).

We will evaluate both Equations 7 and 8 using data from Tables 1 and 2, starting with Equation 7. We will use Equation 3 to calculate v_{tan}, which we need to evaluate Equation 7.

This time, s in Equation 3 represents the space distance traveled by one of the binary components in time t, r represents the distance to the component, and, to avoid confusion with position angle, we replace θ with α, which represents the angular distance through the sky that the component travels in time t. Taking the time derivative of Equation 3 gives,

Equation 9 $$\frac{ds}{dt} = r\,\frac{d\alpha}{dt}\,,$$

Where $\frac{ds}{dt}$ is the tangential component, v_{tan}, of the space velocity of one of the stars, r is the distance to the star, and $\frac{d\alpha}{dt}$ is the proper motion of the star.

For the primary:

r = 1/[parallax (arcsecs)] = 65.12 parsecs = 2.019×10^{15} km.

$$\frac{d\alpha}{dt} = 45.27 \text{ mas/yr} = 6.95 \times 10^{-15} \text{ radians/sec}$$

$$v_{tan,Pri} \text{ (km/s)} = [\text{r (km)}][\frac{d\alpha}{dt} \text{ (radians/sec)}] = 14.04 \text{ km/sec.}$$

For the secondary:

$$r = 1/[\text{parallax (arcsecs)}] = 65.12 \text{ parsecs} = 2.019 \times 10^{15} \text{ km.}$$

$$\frac{d\alpha}{dt} = 44.17 \text{ mas/yr} = 6.78 \times 10^{-15} \text{ radians/sec}$$

$$v_{tan,Sec} \text{ (km/s)} = [\text{r (km)}][\frac{d\alpha}{dt} \text{ (radians/sec)}] = 13.69 \text{ km/sec.}$$

For the relative tangential velocity:

$$\Delta v_{\text{tan}} = v_{tan,Pri} - v_{tan,Sec} = 14.04 \text{ km/sec} - 13.69 \text{ km/sec} = 0.05 \text{ km/sec. Negligible.}$$

Equation 10 $\Delta v_{\text{rad}} = v_{\text{rad,Pri}} - v_{\text{rad,Sec}} = -32.96 \text{ km/sec} - (-34.40 \text{ km/sec}) = 1.440 \text{ km/sec.}$

Ignoring Δv_{tan} (negligible), Equation 7 reduces to $\Delta v_{\text{rel}} = |\Delta v_{\text{rad}}| = 1.440$ km/sec. We want to know how this value compares to the escape relative velocity, Equation 8.

For the escape relative velocity we plug into equation 8 the gravitational constant, $G = 6.674 \times 10^{-11}\ \text{m}^3\ \text{kg}^{-1}\ \text{sec}^{-2}$, the sum of the masses (given above for typical K0V and K2V stars) of the components, $M_{TOT} = 0.78\ M_{SUN} + 0.74 M_{SUN} = 1.52\ M_{SUN} = 2.92 \times 10^{30}$kg, and the space separation (calculated above) of the components, $R = 2.019$ km, which yields

$$\Delta v_{\text{esc}} = 1.35 \text{ km/sec.}$$

$$\Delta v_{rel} \approx \Delta v_{\text{esc}}$$

At the end of the day this pair look a lot less bound than when we started. The escape relative velocity and the relative velocity are about the same. We can get an idea of the chances of boundedness by considering the greatest possible effect of the errors of the relevant quantities, favoring boundedness. That is, how could we apply the errors to their associated quantities such that Δv_{esc} is maximized and Δv_{rel} is minimized?

Main sequence masses inferred from spectral type may be in error by about 15% (Nordstrom 1989). Therefore, the value of M_{TOT} we used previously in Equation 8 may be greater by a factor of 1.15, increasing the resulting value of Δv_{esc}, and tending toward binding the system. But increasing the value of M_{TOT} to 1.15 M_{TOT} yields a maximum likely value of $\Delta v_{\text{esc}} = 1.41$ km/sec. Not much bigger than the previously calculated value of 1.35 km/sec and of little help in binding this system.

Reducing the space separation r would also increase Δv_{esc}, but the error in r (as a result of the parallax error) is negligibly small compared to the other errors involved and would be of little help in increasing Δv_{esc}.

The errors in the radial velocities of the components (Table 2) can similarly be applied to the associated radial velocities in such a way as to minimize $| \Delta v_{rad} | = \Delta v_{rel}$ (Equation 7, ignoring Δv_{tan}), tending toward binding the system. Thus, adding -0.5859 km/sec to $v_{rad,Pri}$ and 1.351 km/sec to $v_{rad,Sec}$, minimizes $| \Delta v_{rad} | = \Delta v_{rel} = 0.7655$ km/sec.

So, to sum up this best-case scenario, where the errors work to favor boundedness, we have

0.7655 km/sec = $\Delta v_{rel} < \Delta v_{esc}$ = 1.41 km/sec.

About all we can conclude from the above examination of the errors is that we cannot rule out boundedness, and if bound, only very loosely.

This pair of stellar birds certainly do flock together, bound or not, but are they of a feather? That is, were they born together within the same fragment of a collapsing cloud core? Fragments that become protostars are typically about 0.1 parsec size. Our pair is separated by about 0.007 parsec, easily fitting within a collapsing fragment. If the components were indeed formed together, we might expect their metallicity to be similar. Metallicity is a measure of a star's iron abundance. Stromgren photometry might answer the question of metallicity and whether the component stars were born together.

6. Photometry

The components of the double, and a comparison star (1626CA3+0211BAL1915), were observed through Stromgren vby filters five times over two nights. Stromgren filters are much narrower than UBV filters and more astrophysical information is obtainable with them than with UBV filters. The v (violet) filter (411 nm) is centered on several strong iron lines.

The (b-y) color index correlates well with surface temperature. The m_1 = (b-v) – (v-y) color index correlates well with metallicity. It is important to note that absorption line strength depends not only on chemical composition of the stellar atmosphere but also on surface temperature. The double star in this work was chosen in part for similarity of spectral-luminosity class between the two components, enabling us to compare m_1 indices without the complications of differing surface temperatures. Differences in m_1 will therefore reflect differences in line strength only, not differences in temperature.

Comparison of instrumental m_1 color indices will tell us what we want to know, which is whether the iron content, or metallicity, of the components is similar. As long as the airmass at the time of observation and the spectral types are the same for all three stars, the differences between those stars in instrumental m_1 color index will be the same as the differences in transformed m_1 color index. Because all three stars are at roughly the same distance (based on spectral-luminosity class and visual magnitude) and are of similar spectral type, interstellar reddening will have about the same effect on all three and therefore differences between instrumental m_1 and transformed m_1 will be unaffected.

Presented in Table 3 are the photometric data for the double star and the comparison.

Table 3. Photometric Data (Instrumental)

Star	Sp. Type	(b-y)	m_1
Primary	K0V	0.9928	-4.3252
Secondary	K2V	1.0486	-4.5702
1626CA3+0211BAL1915	K2V	1.0438	-4.3594

The first thing to notice is the consistency of (b-y) with WDS spectral type. All three values are very close to equal, and the K0V, being slightly hotter, is slightly bluer in (b-y), as expected. The WDS spectral types are still holding up.

What really sticks out is the dissimilarity in values of $m_{1,}$ which reflects differences in metallicity, for the primary and secondary. For a given (b-y), a difference in m_1 of a couple of tenths of a magnitude can mean a difference in iron to hydrogen ratio of 50 – 100 % (e.g., Arnadottir et al. 2010).

Also remarkable is the m1 value for the comparison (BAL1915). This star is unrelated to the double under study, but was selected for its similar spectral-luminosity class, visual magnitude (= 10.16) and position. Its position puts it at nearly the same airmass as the double, at time of observation. The comparison just happens to have nearly the same m_1 value as the primary but is at least two degrees away and clearly not associated with the primary. This similarity in m_1 between the primary and the comparison is in stark contrast to the surprising *dissimilarity* in m_1 between the primary and secondary. I expected them to be of common origin and co-chemical. Clearly the primary and secondary did not form from the same cloud core fragment, or their compositions would be similar.

The components of physical doubles do not have to form from the same cloud core fragment. Wide binaries can form from adjacent, collapsing cloud cores, if they are moving slowly enough with respect to one another (e.g., Tokovinin et al. 2017). Wide binaries can also form during the dissolution phase of young star clusters (e.g., Kouwenhoven et al. 2010). In neither case do we expect similar metallicity, and so our double, if bound, may have formed in one of those two ways.

7. Conclusion

The pair of stellar birds under study certainly flock together, as indicated by their similar proper motions and radial velocities, but are of dissimilar metallicity and therefore did not form together and are *not* of a feather.

It is unlikely the pair is bound but, on that score, these stellar birds just refuse to be pigeon holed. Only if the errors are distributed over their associated radial velocities in the most favorable possible way would the components be bound. In his table, Harshaw (2018) calculates a probability of boundedness for this double of 89.5%. I am somewhat less optimistic. I would move his decimal point one place to the left.

The considerable time and effort invested in this double over the last 120 years would be much better spent on a pair with a much shorter period. It is extremely hard to test observationally whether wide binaries are gravitationally bound, because of their long periods. With Gaia parallaxes so readily available, and many periods therefore estimable, many wide binaries in the WDS can be ruled out as worthwhile targets.

8. References

1. Arnadottir, A.S., Feltzing, S., Lundstroem, I., “The Ability of Intermediate-Band Stromgren Photometry to Correctly Identify Dwarf, Subgiant, and Giant Stars and Provide Stellar Metallicities and Surface Gravities,” *A&A*: 521, id.A40, 34.
2. Harshaw, R., 2018, “Gaia DR2 and the Washington Double Star Catalog: A Tale of Two Databases,” *JSDO*: 14(4), 734 – 740.
3. Kouwenhoven, M. B. N., Goodwin, S.P., Parker, R. J., Davies, M. B., Malmberg, D., Kroupa, P., 2010, “The Formation of Very Wide Binaries During the Cluster Dissolution Phase,” *MNRAS*: 404(4), 1835 – 1848.
4. Mason, B., 2017, *The Washington Double Star Catalog*, Astrometry Department, U.S. Naval Observatory.
5. Nordstrom, B., 1989, “On “The” Spectral Type-Mass Relation for Main-Sequence Stars,” *Ap. J.*: 341, 934 – 938.
6. Sinachopoulos, D. & Van Dessel, E. 1992, “Stromgren Photometry of Wide Visual Double Stars with G-Type Primaries, Most of Which Have Common Origin Components,” *Complimentary Approaches to Double and Multiple Star Research, IAU Colloquium 135, ASP Conference Series, Vol 32, Harold A. McAlister and William I. Hartkoph (eds.).*
7. Tokovinin, A., 2017, “Formation of Wide Binary Stars from Adjacent Cores,” *MNRAS*: 000, 1 – 6.
8. Zombeck, M., (1990), *Handbook of Space Astronomy and Astrophysics (2nd ed.),* Cambridge University Press, ISBN 978-0-521-34787-7.